O_3-NO_x-VOC sensitivity and NO_x-VOC indicators in Paris: Results from models and Atmospheric Pollution Over the Paris Area (ESQUIF) measurements

Sanford Sillman,[1] Robert Vautard,[2] Laurent Menut,[3] and Dieter Kley[4]

Received 3 December 2001; revised 25 August 2002; accepted 21 September 2002; published 18 June 2003.

[1] A three-dimensional photochemical model has been used to interpret aircraft measurements from the Atmospheric Pollution Over the Paris Area campaign near Paris, with special attention to measurements that are related to predicted O_3-NO_x-volatile organic compound (VOC) sensitivity. The model (CHIMERE) includes a representation of ozone formation over Europe and a more detailed spatial representation of the region around Paris. A series of model scenarios were developed with varying wind speeds and emission rates. Comparisons are shown with measured O_3, total reactive nitrogen (NO_y), summed VOCs, and isoprene. Results show that model NO_x-VOC sensitivity predictions are correlated with the ratio O_3/NO_y but not with O_3/peroxyacetyl nitrate. Measured O_3 and NO_y on high-ozone days tends to agree with model values when models predict NO_x-sensitive or transitional chemistry but not when models predict VOC-sensitive chemistry. Model values for O_3/NO_y and the O_3-NO_y slope are lower than measured values, suggesting the possibility of missing, unmeasured VOCs in the Paris plume. Standard performance tests for ozone models, such as normalized bias, show good agreement between models and measurements, even in cases when significant differences appear in the O_3-NO_y correlation. Model predictions shift slightly toward NO_x-sensitive chemistry when model wind speeds are increased. Isoprene represents 20% of total VOC reactivity–weighted carbon in the center of the Paris plume and 50% in the surrounding rural area during high-ozone events. *INDEX TERMS:* 0315 Atmospheric Composition and Structure: Biosphere/atmosphere interactions; 0345 Atmospheric Composition and Structure: Pollution—urban and regional (0305); 0365 Atmospheric Composition and Structure: Troposphere—composition and chemistry; *KEYWORDS:* ozone, nitrogen oxides, VOCs, isoprene, photochemical models

Citation: Sillman, S., R. Vautard, L. Menut, and D. Kley, O_3-NO_x-VOC sensitivity and NO_x-VOC indicators in Paris: Results from models and Atmospheric Pollution Over the Paris Area (ESQUIF) measurements, *J. Geophys. Res.*, *108*(D17), 8563, doi:10.1029/2002JD001561, 2003.

1. Introduction

[2] It is generally thought that in the densely populated regions of northern Europe, ozone is more likely to be sensitive to emissions of volatile organic compounds (VOCs) than to NO_x. Previous model-based studies of pollution events in northern Europe have found that ozone chemistry is limited by the availability of VOC and that biogenics have a minor impact, although there is considerable uncertainty [*Simpson*, 1995]. The situation in northern Europe stands in contrast with results from southern Europe and parts of the eastern U.S., where ozone is often sensitive to NO_x rather than to VOC and where biogenics have a significant impact [e.g., *Chameides et al.*, 1988; *Sillman et al.*, 1995; *Staffelbach et al.*, 1997a, 1997b].

[3] The recent Atmospheric Pollution Over the Paris Area (ESQUIF) field measurements provide an opportunity to examine predicted O_3-NO_x-VOC sensitivity in comparison with measurements. The ESQUIF project, described elsewhere [*Menut et al.*, 2000b; *Vautard et al.*, this issue], includes aircraft measurements of O_3, speciated VOCs, and total reactive nitrogen (NO_y). NO_y is especially important because previous investigations have suggested that measured NO_y can be used as an "indicator" for O_3-NO_x-VOC sensitivity. Results from both models and measurements suggest that the ratio O_3/NO_y has a relatively low value during VOC-sensitive conditions and a high value during NO_x-sensitive conditions [*Sillman*, 1995; *Sillman et al.*, 1998; *Sillman and He*, 2002]. Measured values of this ratio provide an indirect way of evaluating model predictions for NO_x-VOC sensitivity. This type of correlation is also

[1]Department of Atmospheric, Oceanic, and Space Sciences, University of Michigan, Ann Arbor, Michigan, USA.
[2]Laboratoire de Meteorologie Dynamique, Ecole Polytechnique, Palaiseau, France.
[3]Laboratoire Inter-Universitaire des Systèmes Atmosphériques, Centre National de la Recherche Scientifique, Cretéil, France.
[4]Forschungszentrum Jülich, Jülich, Germany.

Copyright 2003 by the American Geophysical Union.
0148-0227/03/2002JD001561

subject to large uncertainties and is not necessarily applicable to all locations [*Lu and Chang*, 1998].

[4] Here we show results from model calculations and ESQUIF measurements that relate to the NO_x-VOC sensitivity in the Paris urban plume. We will use a three-dimensional (3D) photochemical transport model (CHIMERE) to represent ozone formation and transport over continental Europe, with finer resolution for the Paris area. A series of model scenarios will be developed based on uncertainties that might affect NO_x-VOC predictions. Correlations between model species concentrations and NO_x-VOC sensitivity predictions will be examined to see whether the previously identified indicators can be correlated with NO_x-VOC sensitivity in this case. Comparison with measured reactive nitrogen and VOCs will be used to identify model biases and to address the issue of uncertainties associated with NO_x-VOC chemistry.

[5] The model and measurements are described in section 2. Section 3 presents correlations between O_3 and reactive nitrogen from various model scenarios and results concerning the abilities of these species to act as indicators for O_3-NO_x-VOC sensitivity. Section 4 shows measured correlations between O_3 and NO_y in comparison with model results, along with other model-measurement comparisons. Section 5 discusses other issues and uncertainties, including the impacts of isoprene and of wind speed on ozone chemistry.

2. Methods

[6] The photochemical model (CHIMERE) and ESQUIF measurements are both described in detail elsewhere [*Vautard et al.*, 2001; *Menut et al.*, 2000b; *Vautard et al.*, this issue]. A brief description is given here.

2.1. ESQUIF Project

[7] About a fifth of the French population lives in the vicinity of Paris, over an area of $\sim$12,000 km^2. As in many urbanized areas, the Paris area frequently has elevated pollutant levels, including high ozone in summer. One of the purposes of the ESQUIF project is to quantify the rate of production of ozone within the region and also to identify transport from distant emission sources. During the summers of 1998, 1999, and 2000, 12 intensive observation periods (IOPs) were carried out to document the dynamical and chemical processes in the region. These IOPs included both a network of surface measurements and numerous aircraft-based measurements. As the Paris area presents a circular form (from the most important surface emissions at the center to rural areas at its boundaries), and as it is far from other major cities or emission sources, the aircraft measurements were made along flight paths that looped around the Paris urban center. The aircraft range and altitude varied from day to day based on aircraft capabilities, local meteorology, and the predicted pollution event.

2.2. Model

[8] A 3D Eulerian model (CHIMERE) [*Vautard et al.*, 2001; *Schmidt et al.*, 2001; *Vautard et al.*, this issue] is used to simulate photochemistry and transport of pollutants within the boundary layer. We only briefly describe the model characteristics here, referring the reader to the previous papers for further details.

[9] The model domain is designed with two subsections. The first, a continental-scale subsection, is used to model chemistry and transport over western and central Europe, with a horizontal resolution of 0.5°. The second, an urban/regional subsection, is used to model the behavior of pollutants over the Paris area. It represents a 150 $\times$ 150 km region centered on Paris, with a horizontal resolution of 6 $\times$ 6 km. Pollutant concentrations from the continental-scale subsection are used as boundary conditions for the regional-scale subsection (one-way nesting).

[10] For both subsections the CHIMERE model consists of five vertical layers, including a surface layer (0–50 m) and upper layers with 500–1000 m thicknesses. Vertical diffusion is estimated as eddy diffusion, based on a Richardson-number-profiles methodology and linearly depending on the boundary layer depth.

[11] These dynamical parameters, wind components, temperature, specific humidity, cloudiness, and pressure, are all derived from the European Centre for Medium-Range Weather Forecasts (ECMWF) model (10 vertical hybrid levels from ground to 700 hPa with a 3 h time resolution). Photochemistry is represented by the MELCHIOR mechanism [*Lattuati*, 1997; *Schmidt et al.*, 2001] and includes gas-phase reactions only. The equations of chemistry and transport are solved using the TWOSTEP solver [*Verwer and Simpson*, 1995], where all processes are solved all together to avoid well-known splitting-operators problems.

[12] Anthropogenic emissions were derived from several databases [*Menut et al.*, 2000a; *Vautard et al.*, 2001]. An updated speciation of VOCs was used for this study [R. Friedrich, IER, University of Stuttgart, private communication, 2001; see also *Vautard et al.*, this issue]. Emissions were also modified to reflect differences between weekdays, Saturdays, and Sundays using urban diurnal profiles deduced from measurements from the AIRPARIF network [*Vautard et al.*, this issue]. In addition, studies of traffic patterns in Paris suggest that substantially lower traffic occurs during Saturdays in August than at other times. This August traffic pattern has not been used in the standard model scenario, but a separate scenario has been created that includes the August traffic pattern as a basis for emissions on Saturdays. Emissions of isoprene and α-pinene were included based on the work of *Derognat et al.* [this issue]. Nitric oxide biogenic emissions due to biological processing of fertilizers in the soils are also considered, following the methodology of *Stohl et al.* [1996]. The model was exercised for a 3 week period in July 1999. Results will be shown here for 16, 17, and 18 July in comparison with measurements.

2.3. Model Scenarios

[13] A series of scenarios with alternate base case emissions will be developed, including the following: (1) the initial scenario, based on emissions and meteorology described above; (2) scenarios with anthropogenic VOC increased by 40% and with NO_x reduced by 30% relative to the inventory values; (3) scenarios with isoprene emission rates doubled relative to the inventory values; (4) scenarios with wind speeds increased by 25% and 75% relative to the original meteorology; and (5) scenarios with the height of the afternoon mixed layer increased by 25% relative to the original meteorology. The scenarios with increased VOC and reduced NO_x were developed based on the uncertainty of

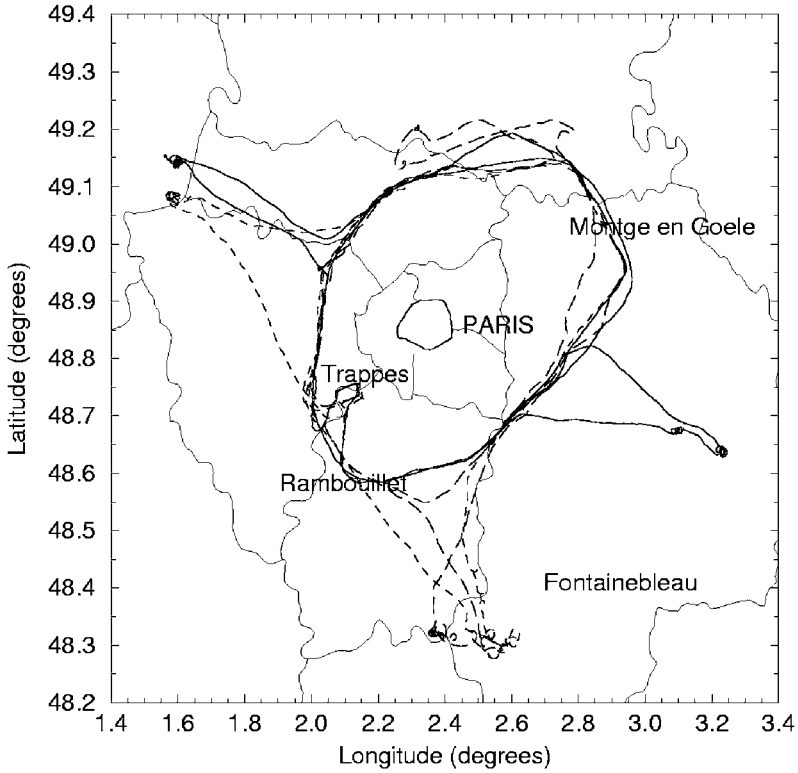

Figure 1. Flight paths of the DIMONA aircraft on 16 July 1999 (solid line), 17 July 1999 (long-dashed line), and 18 July 1999 (short-dashed line). The shaded solid lines are the boundaries of French departments.

VOC and NO_x emissions, estimated as ±40% [*Beekmann and Derognat*, this issue; *Vautard et al.*, this issue]. *Vautard et al.* [this issue] also provide cases with different NO_x-VOC sensitivity from the initial scenario. As in previous studies of this type [*Sillman et al.*, 1995, 1998], scenarios with different predicted NO_x-VOC sensitivities will be used to evaluate uncertainty in model predictions and to identify whether comparisons with measurements can reduce this uncertainty. The scenarios with higher wind speeds reflect uncertainties in winds during the event. Because winds are generally light during the period (2 m s^{-1} or less), a 25% change is likely within the range of uncertainty associated with wind measurement and interpolation. A scenario with 75% higher wind speeds was added in order to identify the impact of wind speed on NO_x-VOC sensitivity. The scenarios with higher daytime mixed layers are based on lidar measurements reported by *Vautard et al.* [2003], which suggest that the height of the afternoon mixed layer may be higher than originally estimated. A scenario with emissions on 17 July modified based on the changes observed in traffic patterns on Saturdays in August [*Vautard et al.*, 2001] has been added, as described above.

[14] Along with each scenario, control strategy simulations will be performed with 30% reductions in either anthropogenic VOC or NO_x emissions relative to the base case. These control scenarios will be used to identify the NO_x-VOC sensitivity of each case.

2.4. Measurements

[15] Measured reactive nitrogen and VOCs are shown from the flights of the DIMONA aircraft [see *Konrad and Volz-Thomas*, 2000]. The aircraft flew a perimeter around Paris at a distance ~30 km from the city center and at an altitude of ~600 m above ground level. Measurements from three flights are studied in this paper: (1) 16 July 1999 at 1135–1536 local standard time (LST); (2) 17 July 1999 at 1416–1824 LST; and (3) 18 July 1999 at 1216–1615 LST. Flight trajectories are shown in Figure 1.

[16] NO_y and peroxyacetyl nitrate (PAN) were measured by the "NO_xTO_y" instrument [*Kanter et al.*, 2001], which was also used and validated during the BERLIOZ campaign. Speciated VOCs (C4–C10) were measured by the Airmotec HC-1010 gas-phase chromatograph [*Konrad and Volz-Thomas*, 2000]. The VOC measurements represent average ambient values over 10 min intervals. O_3 and reactive nitrogen represent instantaneous measurements at 10 s intervals.

3. Model NO_x-VOC Sensitivity and Indicator Ratios

[17] The relation between total reactive nitrogen and O_3-NO_x-VOC sensitivity in Paris is shown in Figure 2. Figure 2 shows a composite plot of O_3 versus NO_y from several model scenarios, including both predominantly VOC-sensitive and NO_x-sensitive cases. Results are shown for several days at afternoon hours corresponding with measurements. Figure 2 also shows each location categorized as VOC-sensitive, NO_x-sensitive, or mixed based on the predicted response of model O_3 to a 30% reduction in emissions of anthropogenic VOCs or NO_x. The categorization of model

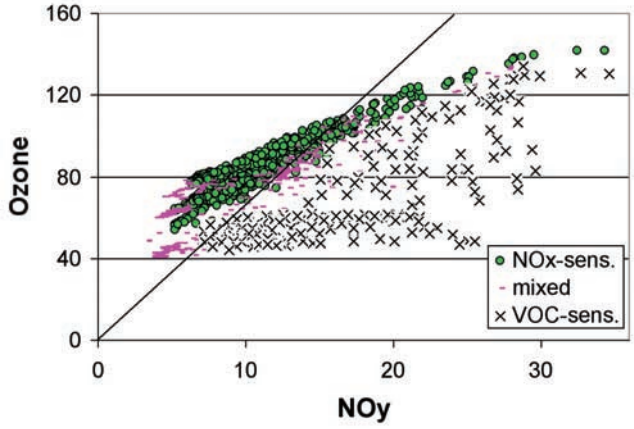

Figure 2. Composite O_3 versus NO_y (ppb) in CHIMERE simulations for 16 July (1400 LST), 17 July (1600 LST), and July 18 (1600 LST) 1999 for scenarios with different predicted NO_x-VOC sensitivities. Locations are classified as NO_x-sensitive (green circles), VOC-sensitive (crosses), and mixed or with near-zero sensitivity (pink points) based on the predicted impact of reduced NO_x and VOCs at that location and hour. The line represents an O_3/NO_y ratio of 6.5.

locations is based on definitions similar to those used in previous studies of this type [*Sillman*, 1995; *Sillman et al.*, 1998]. Simulated O_3 at a specific time and location are compared for a model base case, for a scenario with 30% reduced anthropogenic VOC emissions, and for a scenario with 30% reduced NO_x. Locations are classified as NO_x-sensitive for a specified hour if O_3 in the scenario with 30% reduced NO_x is lower than O_3 in both the base case and in the scenario with 30% reduced VOCs by at least 2 ppb. Locations are classified as VOC-sensitive if O_3 in the scenario with reduced VOCs is lower than O_3 in the other scenarios by at least 2 ppb. Locations that are neither VOC-sensitive or NO_x-sensitive by this definition are classified as having mixed sensitivity if O_3 in the scenarios with reduced NO_x and with reduced VOCs is lower than O_3 in the base case by at least 2 ppb; locations are classified as insensitive to NO_x and VOC otherwise. This definition differs from those used previously only in that the threshold for defining NO_x and VOC sensitivity has been lowered to 2 ppb for the Paris case.

[18] As shown in Figure 2, NO_x-sensitive and VOC-sensitive locations are associated with a different range of values of O_3 and NO_y. NO_x-sensitive locations have higher O_3/NO_y ratios and tend to occupy a relatively narrow range of O_3 and NO_y values, with O_3 increasing with increasing NO_y. VOC-sensitive locations have lower O_3/NO_y ratios and occur over a wider range of O_3 and NO_y. There is also less correlation between O_3 and NO_y among VOC-sensitive locations in this composite plot, but individual VOC-sensitive events may still show a positive correlation between O_3 and NO_y. The connection between model reactive nitrogen and NO_x-VOC sensitivity is consistent with previous results in the U.S.

[19] Previously, *Sillman* [1995] expressed the above relationship in terms of the ratio O_3/NO_y. NO_x-sensitive locations were identified with O_3/NO_y above a certain transition value (6.5 in this case), and VOC-sensitive locations were identified with O_3/NO_y below the transition value. A line representing the transition value has been superimposed in Figure 2. It is apparent that the O_3/NO_y ratio and the transition value is an imperfect representation of the relation between model O_3, NO_y, and NO_x-VOC sensitivity. At low O_3 and NO_y, VOC-sensitive conditions persist for O_3/NO_y somewhat higher than the transition value, while at higher O_3 and NO_y, NO_x-sensitive conditions persist for somewhat lower O_3/NO_y. A similar pattern of variation was found in model results from the U.S. [*Sillman and He*, 2002]. The transition value is also sensitive to the level of background O_3 and NO_y [see *Sillman and He*, 2002]. Though imperfect, the ratio provides a concise way for summarizing the relation between reactive nitrogen and NO_x-VOC sensitivity in models.

[20] *Sillman et al.* [1998] identified the NO_x-VOC transition value for O_3/NO_y and other indicator ratios by examining the percentile distribution of O_3/NO_y among model NO_x-sensitive and VOC-sensitive locations. The 95th percentile value for VOC-sensitive locations and the 5th percentile value for NO_x-sensitive locations were interpreted to show the value associated with the transition from VOC-sensitive to NO_x-sensitive chemistry. Table 1 shows the results for the Paris simulation in comparison with previous results for simulations in the U.S. (Nashville, Tennessee). Results show that O_3/NO_y and the other indicator ratios behave similarly in the Paris simulations as in the previously reported cases discussed by *Sillman et al.* [1998]. The transition values for indicators in the Paris simulations are similar to the values reported for Nashville in simulations with similar dry deposition for HNO_3 (2.5 cm s^{-1}). Slightly higher transition values were found for Nashville in simulations with higher dry deposition (see Table 1).

[21] A similar pattern to Figure 2 is also found for O_3 versus NO_z (defined as NO_y-NO_x) and for O_3 versus HNO_3. These are summarized in transition value statistics shown in Table 1. However, the correlation between O_3 and PAN behaves differently. As shown in Figure 3, O_3 versus PAN is not correlated with model NO_x-VOC sensitivity. O_3 is positively correlated with PAN in models, and the correlation varies from day to day (due to changes in temperature). The same values of O_3 and PAN appear for both NO_x-sensitive and VOC-sensitive locations. The correlation between NO_x-VOC sensitivity and O_3/NO_y, illustrated in Figure 2, is driven specifically by HNO_3 (and, to a lesser extent, by NO_x) rather than by PAN and other organic nitrates. This is consistent with the radical chemistry associated with NO_x-VOC sensitivity (see the summary by *Sillman* [1999]) and with results from the work of *Tonnesen and Dennis* [2000].

4. Model-Measurement Comparisons

4.1. O_3 and NO_y

[22] Figure 4 shows comparisons between model and measured O_3 and NO_y on 17 July (1600 LST) for three model scenarios: the standard scenario (VOC-sensitive), the scenario with higher VOC and lower NO_x emissions (NO_x-sensitive), and the scenario with higher VOC emissions and with the daytime mixed layer increased by 25% (mixed sensitivity). As in the previous figures, model values have been categorized as NO_x-sensitive, VOC-sensitive, or mixed

Table 1. Percentile Distribution of Indicator Values in NO_x-Sensitive and VOC-Sensitive Locations[a]

	VOC-Sensitive Locations			NO_x-Sensitive Locations		
	5th Percentile	50th Percentile	95th Percentile	5th Percentile	50th Percentile	95th Percentile
			O_3/NO_y			
Paris	3.0	4.7	5.5	6.3	8.8	12.0
Nashville, low deposition	2.2	3.6	5.6	7.1	10.8	13.0
Nashville, high depositon	2.6	5.3	7.2	8.7	13.9	17.0
			O_3/NO_z			
Paris	5.2	6.1	7.8	7.0	10.4	15.0
Nashville, low deposition	5.3	6.3	7.3	8.4	12.4	13.0
Nashville, high deposition	7.0	8.8	9.9	10.5	16.8	20.0
			O_3/HNO_3			
Paris	11.0	12.0	14.0	14.0	18.0	26.0
Nashville, low deposition	6.0	8.0	9.0	12.0	19.0	21.0
Nashville, high deposition	8.0	11.0	14.0	15.0	25.0	29.0
			$H_2O_2//HNO_3$			
Paris	0.11	0.16	0.27	0.29	0.43	0.73
Nashville, low deposition	0.11	0.18	0.23	0.30	0.64	0.82
Nashville, high deposition	0.09	0.15	0.21	0.26	0.55	0.70

[a]Shown are 5th percentile, 50th percentile, and 95th percentile indicator values (with percentile ordering by indicator value) for VOC-sensitive locations and for NO_x-sensitive locations as defined in the text. Results from the Paris standard scenario (at 1600 LST, 17 July) are compared with results from Nashville scenarios with low deposition (2.5 cm s^{-1} for H_2O_2 and HNO_3) and with high deposition (5 cm s^{-1}) [*Sillman et al.*, 1998].

based on the predicted sensitivity at each location for the given hour. Results associated with peak O_3 for each scenario are also shown in Table 2.

[23] Results show that predicted NO_x-VOC sensitivity varies considerably among the three model scenarios. The initial scenario predicts VOC-sensitive chemistry throughout the Paris urban plume. NO_x-sensitive chemistry is associated with lower O_3 and NO_y along the plume outskirts or in the surrounding rural region. The scenario with increased VOC and decreased NO_x emissions predicts NO_x-sensitive chemistry almost everywhere, even for locations near the city center. The scenario with higher VOC emissions and increased wind speeds predicts mixed sensitivity, with VOC-sensitive conditions near the city center, NO_x-sensitive conditions at downwind and rural locations, and equal sensitivity to NO_x and VOC in the plume locations with highest O_3. These varying NO_x-VOC predictions occur despite the fact that O_3 is similar in all three scenarios.

[24] Comparison between models and measurements show good agreement only when the model predicts mixed or NO_x-sensitive chemistry. A strong correlation between O_3 and NO_y is predicted for the NO_x-sensitive subregion in all three model scenarios, and this correlation matches visually with measurements. By contrast, the VOC-sensitive locations in the standard scenario differ substantially from measured values. Peak O_3 in the standard scenario is slightly lower than measured peak O_3 (131 ppb modeled, 142 ppb measured); NO_y concurrent with peak O_3 is significantly higher (33 ppb modeled, 21 ppb measured), and O_3/NO_y is much lower (4.0 ppb modeled, 6.8 ppb measured) (see Table 2). The NO_x-sensitive and mixed scenarios have similar peak O_3 to the standard scenario but with lower NO_y. These agree more closely with measured peak O_3 and NO_y, though O_3/NO_y (4.7–5.0) is still underestimated. Correlation statistics (Table 3) show that the rate of increase of O_3 with NO_y is underestimated in all model scenarios. The underestimate is smaller in the NO_x-sensitive scenario but even here, the model O_3-NO_y slope is 25% lower than the measured slope.

[25] Measurements on 18 July (Figure 4d) also show a strong correlation between O_3 and NO_y, with slightly higher O_3 for equivalent NO_y compared to 17 July. The standard model scenario predicts NO_x-sensitive conditions in most of the Paris plume (though with mixed NO_x-VOC sensitivity in the plume center with highest O_3) and a strong correlation between O_3 and NO_y. In contrast with 17 July the model tends to underestimate O_3 relative to NO_y throughout the entire region, not just in the Paris plume. The model also underestimates the rate of increase of O_3, with NO_y somewhat relative to measured values (see Table 3). Measurements on 16 July (Figure 4e) show a different pattern, with

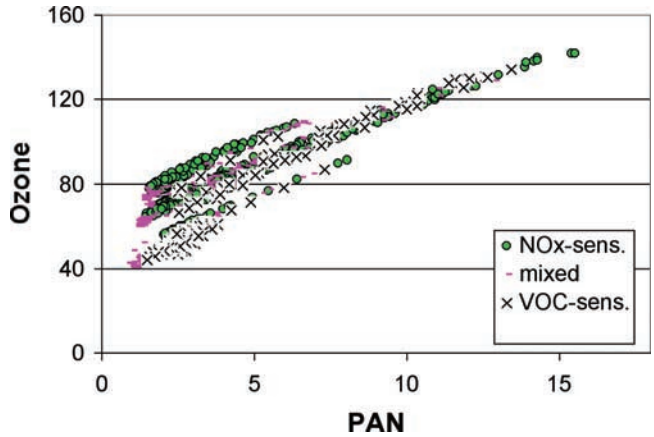

Figure 3. Same as in Figure 2, but for composite O_3 versus peroxyacetyl nitrate (PAN) (ppb).

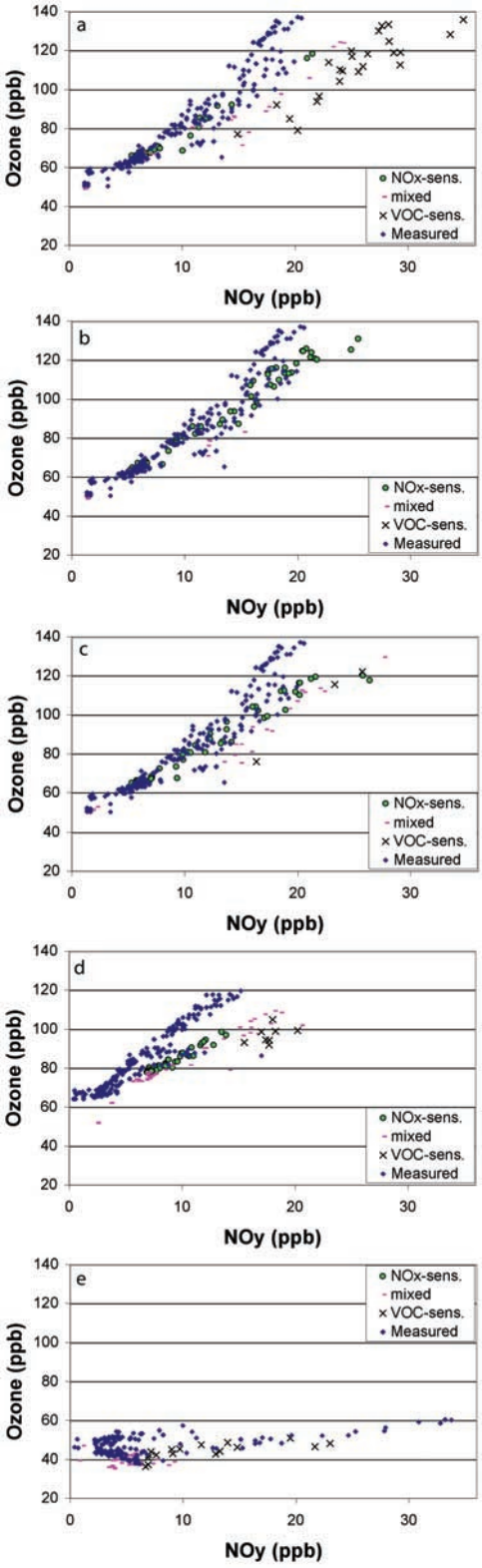

much lower O_3, higher NO_y, a low O_3-NO_y slope, and likely VOC-sensitive chemistry. The model standard scenario predicts VOC-sensitive chemistry throughout the domain and shows good agreement with O_3 versus NO_y.

[26] Figure 5 shows a comparison between O_3 and NO_y in Paris on 17 and 18 July with previously measured O_3 and NO_y in urban plumes in Atlanta, Georgia, and in Nashville [*Sillman et al.*, 1995, 1998]. As shown in Figure 5, the observed pattern of O_3 and NO_y in Paris on 18 July is similar to the previous observations in Nashville in terms of both magnitude and the O_3-NO_y slope (see also Figure 2). The O_3-NO_y slope in Paris on 17 July is similar to the O_3-NO_y slope on 18 July but with higher NO_y for equivalent O_3. The O_3/NO_y ratio concurrent with peak O_3 in Paris (6.8 on 17 July, 7.9 on 18 July) is somewhat lower than peak O_3/NO_y in Nashville (8.4). The O_3/NO_y ratio in Paris is much lower than the equivalent O_3/NO_y in Atlanta (11–16) and is much higher than in Los Angeles, California (3.6 [*Sillman et al.*, 1997]). Measured O_3/NO_y in Atlanta and in Los Angeles represent the likely extreme values associated with NO_x-sensitive and VOC-sensitive chemistry, respectively, while the intermediate value at Nashville was associated with intermediate NO_x-VOC chemistry. O_3/NO_y concurrent with peak O_3 in Paris on 16 July was also very low (1.9).

4.2. Spatial Distribution and Other Species

[27] Ozone in the region forms in a coherent plume extending downwind from the Paris urban center. This spatial pattern appears in both the model and in the measurements (see *Vautard et al.* [this issue] for more details). The location of the downwind plume in the model is generally consistent with aircraft measurements. This is illustrated in Figure 6, which shows model and measured species along the aircraft flight path on 17 July. Elevated O_3, NO_y, and anthropogenic VOCs appear when the aircraft flight path intersects with the Paris urban plume. The location and structure of these plumes is generally consistent between model and measurements. The underestimate of NO_y in the urban plume in the model base case is also evident in Figure 6.

[28] Figure 7 and Table 4 show the correlation between summed anthropogenic VOCs and NO_y from measurements and from the standard model scenario along the aircraft trajectory for 17 July. Summed VOCs have been expressed as propene-equivalent carbon [*Chameides et al.*, 1992], a sum in which each primary VOC species is weighted by its

Figure 4. (opposite) Measured O_3 versus NO_y (ppb) (blue diamonds) compared with model results. Model values are classified as NO_x-sensitive (green circles), VOC-sensitive (crosses), and mixed or with near-zero sensitivity (pink points) based on the predicted impact of reduced NO_x and VOCs at that location and hour. The results are for (a) 17 July 1999 (1600 LST) with a standard model scenario, (b) 17 July 1999 with a scenario with increased VOCs and lowered NO_y, (c) 17 July 1999 with wind speeds increased by 25%, (d) 18 July 1999 (1600 LST) with a standard scenario, and (e) 16 July 1999 (1400 LST) with a standard scenario. Linear least squares coefficients are shown in Table 3.

Table 2. Peak O_3, NO_y, and Predicted NO_x-VOC Sensitivity in Paris[a]

	16 July 1999 (1400 LST)				17 July 1999 (1600 LST)				18 July 1999 (1600 LST)			
	Peak O_3	NO_y	Reduced VOCs	Reduced NO_x	Peak O_3	NO_y	Reduced VOCs	Reduced NO_x	Peak O_3	NO_y	Reduced VOCs	Reduced NO_x
Measured	60	34			143	21			120	15		
Model scenario[b]												
Standard	59	9–18	6	−10	131	33	24	9	109	17	6	7
Weekend adjustment					129	30	17	11	105	15	4	8
Higher VOCs					142	34	11	15	115	18	5	10
High VOCs, low NO_x					126	25	3	13	105	14	2	8
25% higher wind					119	24	15	10	101	14	4	6
25% higher wind and double isoprene					121	24	14	11	103	15	4	7
25% higher wind and higher VOCs					126	27	12	13	107	18	5	8
75% higher wind					108	20	11	9	97	15	4	5
25% higher mixing height					118	25	16	8	104	17	5	6
25% higher mixing height and higher VOCs					127	26	9	13	109	18	4	9

[a]Shown are the following: peak O_3 in the Paris urban plume; NO_y concurrent with peak O_3; the predicted reduction in peak O_3 resulting from a 30% decrease in the emission of anthropogenic VOCs in the Paris region; and the predicted reduction in peak O_3 resulting from a 30% decrease in NO_x. (Negative values represent a predicted increase in O_3 resulting from reduced emissions.)

[b]The model scenarios are: (1) the standard scenario; (2) a scenario with emissions adjusted based on weekend estimates from the work of *Vautard et al.* [2001]; (3) a scenario with anthropogenic VOC emissions increased by 40% relative to scenario 1; (4) a scenario with anthropogenic emissions increased by 40% and NO_x decreased by 30% relative to scenario 1; (5) a scenario with wind speeds throughout the Paris region increased by 25%; (6) scenario 5 with double isoprene emissions; and (7) scenario 5 with anthropogenic VOC emissions increased by 40%. Also shown is O_3 from calculations with 30% reduced anthropogenic VOC and 30% reduced NO_x relative to each scenario base case.

rate of reactivity with OH (normalized relative to propene) and by the number of carbon atoms. Results for individual VOCs are shown in *Vautard et al.* [this issue]. As shown in Figure 7, anthropogenic VOCs and NO_y are generally correlated both in models and in measurements. Peak measured VOC levels are significantly lower than the model maximum values, but this may be the result of the relatively long averaging time (10 min) for the individual measurements. Measured VOCs are higher than model VOCs for equivalent NO_y, but the slope between VOCs and NO_y (Table 4) is slightly lower in the measurements than in the standard model scenario.

[29] Unlike other VOCs, isoprene (Figure 8) does not correlate with NO_y. Model isoprene is generally comparable in magnitude with measured values. However, there is considerable uncertainty over the impact of vertical mixing on isoprene concentrations, as discussed in section 5.

[30] The U.S. Environmental Protection Agency (EPA) uses two statistics to characterize the performance of air quality models: normalized bias, $(1/N)\sum_1^N[(C_m - C_o)/C_o]$, and normalized gross error, $(1/N)\sum_1^N[(|C_m - C_o|)/C_o]$, where C_m and C_o represent model and observed concentrations, respectively. These statistics are shown in Table 5. They show unusually good agreement for O_3 in most of the model scenarios, with the normalized bias <5% and a normalized gross error of 10%. The normalized bias for NO_y is just +12% despite the apparent overestimate of NO_y in Figures 4 and 6. The statistics for summed VOCs

Table 3. Linear Least Squares Coefficients For O_3 Versus NO_y[a]

	16 July 1999 (1400 LST)			17 July 1999 (1600 LST)			18 July 1999 (1600 LST)			Nashville, 13 July 1999 (1400 LST)		
	a_0	a_1	r^2	a_0	a_1	r^2	a_0	a_1	r^2	a_0	a_1	r^2
Measured	44.0	.38	.28	40.0	4.3	.89	58.0	4.0	.89	62.0	4.8	.90
Model scenario[b]												
Standard	41.0	.78	.49	53.0	2.2	.79	63.0	2.1	.68	59.0	3.1	.73
Weekend adjustment				50.0	2.6	.89	60.0	2.6	.78			
Higher VOCs				50.0	2.7	.84	61.0	2.4	.73			
High VOCs, low NO_x				46.0	3.3	.90	57.0	3.0	.80			
25% higher wind				53.0	2.2	.73	63.0	2.1	.62			
25% higher wind and double isoprene				52.0	2.4	.79	64.0	2.2	.62			
25% higher wind and higher VOCs				51.0	2.7	.84	61.0	2.4	.67			
75% higher wind				52.0	2.3	.69	63.0	2.1	.61			
25% higher mixing height				52.0	2.3	.79	60.0	2.4	.74			
25% higher mixing height and higher VOCs				50.0	2.7	.84	58.0	2.6	.74			

[a]Shown are the linear least squares estimators for the linear correlation $[O_3] = a_0 + a_1[NO_y]$ in ppb from Figure 4 along with the correlation coefficient (r^2) from measurements and model scenarios. Results for Nashville (from measurements and models described by *Sillman et al.* [1998]) are shown for comparison.

[b]The model scenarios are: (1) the standard scenario; (2) a scenario with emissions adjusted based on weekend estimates from the work of *Vautard et al.* [2001]; (3) a scenario with anthropogenic VOC emissions increased by 40% relative to scenario 1; (4) a scenario with anthropogenic emissions increased by 40% and NO_x decreased by 30% relative to scenario 1; (5) a scenario with wind speeds throughout the Paris region increased by 25%; (6) scenario 5 with double isoprene emissions; and (7) scenario 5 with anthropogenic VOC emissions increased by 40%. Also shown is O_3 from calculations with 30% reduced anthropogenic VOC and 30% reduced NO_x relative to each scenario base case.

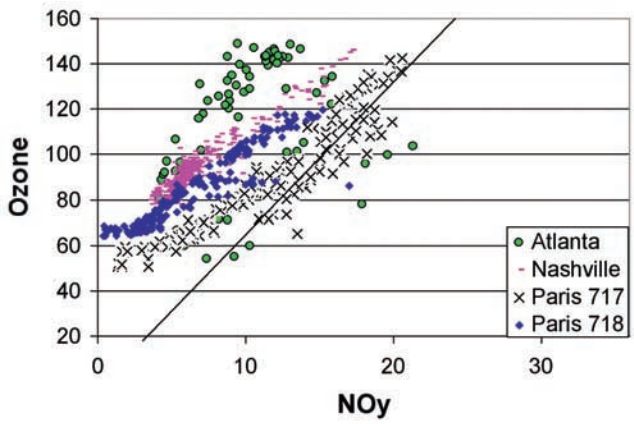

Figure 5. Measured O_3 versus NO_y (ppb) in the Paris plume on 17 July (crosses) and 18 July (blue diamonds) compared with similar measurements in Atlanta, Georgia (green circles), and in Nashville, Tennessee (pink points) [from *Sillman et al.*, 1995, 1998]. The line represents an O_3/NO_y ratio of 6.5.

show a slight underestimate (−21%) in the model standard scenario.

5. Discussion

[31] The results shown in section 4 suggest that ozone chemistry in the Paris plume is often close to the transition between VOC-sensitive and NO_x-sensitive conditions and that the Paris plume may include regions of both NO_x-sensitive and VOC-sensitive chemistry in different locations and on different days. This conclusion is supported by both model and measured O_3 and NO_y. Models predict regions of both NO_x-sensitive and VOC-sensitive chemistry, and predicted NO_x-VOC sensitivity in models varies from day to day. Measured O_3 and NO_y on 17 July are close to the range of values associated with the transition from NO_x-sensitive to VOC-sensitive chemistry in model calculations (e.g., compare Figures 2 and 5). Measurements on 18 July had higher O_3/NO_y ratios, suggesting NO_x-sensitive chemistry, while measurements on 16 July had much lower O_3/NO_y ratios, suggesting VOC-sensitive chemistry. Here we suggest that uncertainties in model predictions may be due to the fact that conditions in Paris are close to the NO_x-VOC transition.

[32] Model measurement comparisons also suggest that the standard model scenarios underestimate the rate of ozone production per NO_x in the Paris urban plume. The ratio O_3/NO_y associated with peak O_3 is underestimated by 40% on 17 July and by somewhat less (24%) on 18 July. This underestimate suggests that the ozone production chemistry may not be sufficiently reactive, possibly because of an underestimate in reactive VOCs. Better agreement between models and measurements can be obtained by using model scenarios with 25% higher wind speeds, higher mixed layer heights, and/or adjusted VOC emissions, but a tendency to underestimate O_3/NO_y remains. Underestimated O_3/NO_y also can be interpreted as evidence that model NO_x-VOC predictions are biased and overestimate sensitivity to VOCs. The slope between O_3 and NO_y (defined as $\Delta O_3/\Delta NO_y$ as opposed to the ratio O_3/NO_y) is underestimated by 15–25% in models relative to measurements. A similar underestimate was found previously for Nashville [*Sillman et al.*, 1998] (see Table 3). From Figure 4, it appears that the underestimated slope on 17 July is associated specifically with the region of peak O_3 and NO_y in the Paris plume, although on 18 July the discrepancy between models and measurements appears over the entire data set.

[33] The most likely cause of this model-measurement discrepancy is an underestimate of VOCs or of VOC reactivity in the Paris plume. However, the underestimated O_3/NO_y in models could also be due to errors associated with the NO_y lifetime and removal. It is possible that reactive nitrogen is removed by dry deposition more rapidly than implied by the model deposition velocity. It is also possible that differences between model and measured NO_y are due to a conversion of reactive nitrogen to aerosol nitrate [*Martilli et al.*, 2002]. Conversion to aerosol nitrate has not been included in the model, and measured NO_y probably does not include aerosol nitrate. It is also possible that measurements underestimate total NO_y due to deposition of HNO_3 along the inlet tube [*Parrish and Fehsenfeld*, 2000; *McClenny*, 2000]. Previously, it was estimated that uncertain deposition rates can cause a 20% uncertainty in O_3/NO_y [*Sillman et al.*, 1998]. *Gao et al.* [1996] also found 20% uncertainties in O_3 associated with uncertain photochemical reaction rates. In the current exercise the discrepancy between measured values and the model standard scenario for 17 July is ~40%, somewhat larger than these uncertainty estimates.

[34] Given these uncertainties, it is especially significant that O_3 and NO_y in the standard model scenario agree with measured values in NO_x-sensitive rural areas and disagree only in the center of the Paris plume, where the model predicts VOC-sensitive chemistry. Possible errors associated with NO_y lifetime and removal or with measurements would cause model-measurement discrepancies over the entire region rather than just in the Paris plume. By contrast, an underestimate in either VOC emissions or reactivity would be consistent with the actual model-measurement discrepancy that appears only in the Paris plume. The discrepancy is much less in model scenarios that have higher mixing heights and more reactive VOCs. These scenarios also move the model in the direction of greater sensitivity to NO_x.

[35] *Vautard et al.* [this issue] found no evidence for errors in either anthropogenic VOC emissions or in the VOC/NO_x ratio, but they found significant uncertainty (±40%) in the emission estimates. In contrast with measured O_3 and NO_y, measured VOCs generally provide evidence

Figure 6. (opposite) Model versus measured species concentrations along the flight trajectory on 17 July (model standard scenario) for (a) O_3 (ppb), (b) NO_y (ppb), (c) summed primary VOCs in propene-equivalents (ppbC), and (d) isoprene (ppb). The solid line represents the model; the points represent measured values. For VOCs and isoprene, the horizontal bars also show the flight interval associated with each measurement, representing a 10 min period.

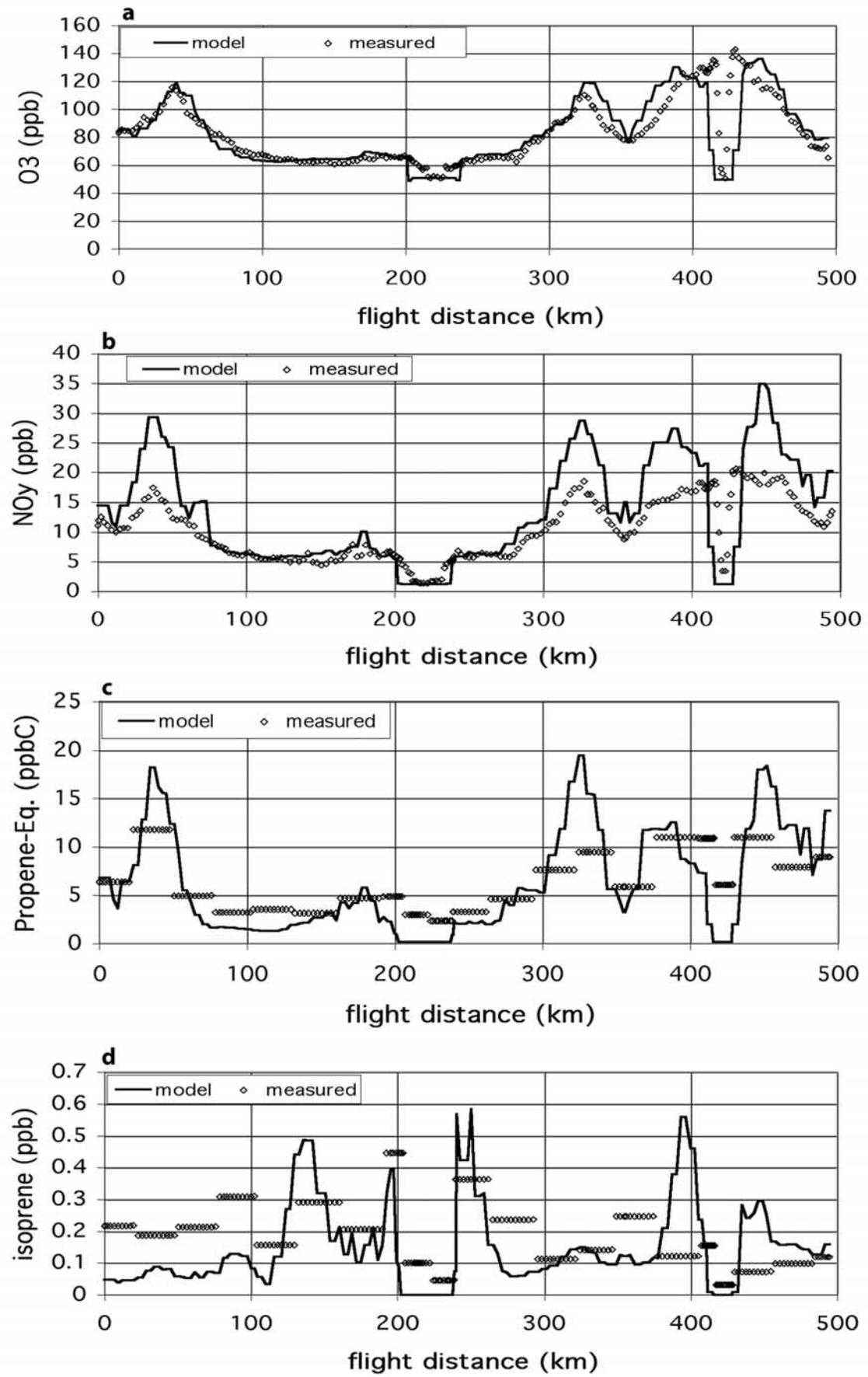
a
model
measured
O3 (ppb)
flight distance (km)
b
NOy (ppb)
c
Propene-Eq. (ppbC)
d
isoprene (ppb)

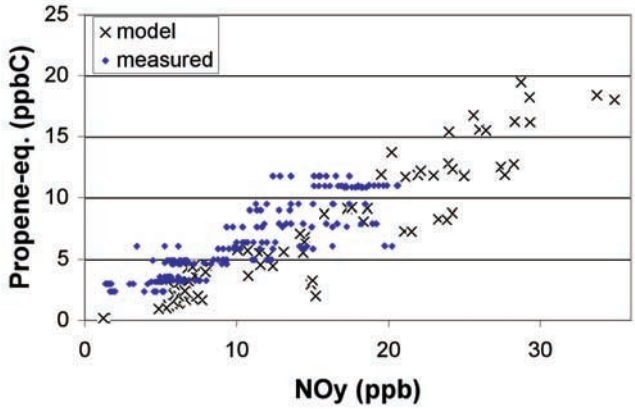

Figure 7. Summed anthropogenic VOCs as propene-equivalent carbon (ppbC) versus NO_y (ppb) in the Paris plume on 17 July from measurements (diamonds) and from the standard model scenario (crosses). Linear least squares coefficients are shown in Table 4.

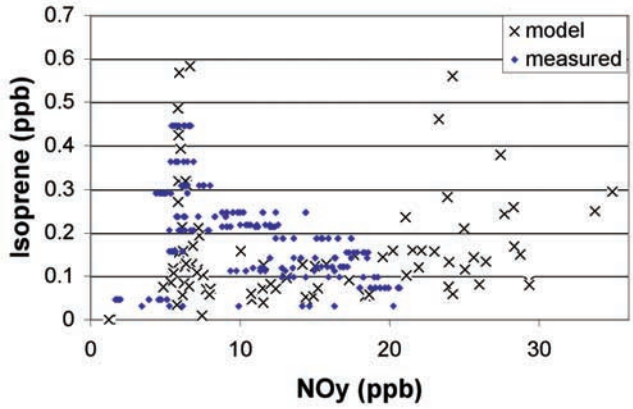

Figure 8. Isoprene versus NO_y (ppb) in the Paris plume on 17 July from measurements (diamonds) and from the standard model scenario (crosses). One ppb isoprene is equal to 19.5 ppbC propene-equivalent carbon.

against the NO_x-sensitive model scenario for 17 July. The NO_x-sensitive scenario requires emission inventories with a higher ratio of VOC/NO_x (or more reactive VOCs) than in the standard scenario. This would cause the model to overestimate the slope between VOCs and NO_y (see Table 4) and overestimate VOCs inside the Paris plume. If the model is underestimating ozone production per NO_x, as suggested above, the underestimate must be associated with VOC species that were not included in the ensemble of ESQUIF measurements.

[36] Emission rates for isoprene have uncertainties of a factor of 2 or more, especially when uncertainties associated with land use and forest composition are included [*Simpson et al.*, 1999]. As shown in Figure 8, isoprene does not correlate with NO_y, and the highest isoprene tends to occur in rural locations with relatively low NO_y. Model isoprene tends to be lower than measured values, although the comparison is inconclusive. The comparison between model and measured isoprene is also inconclusive because the model lacks adequate resolution for representing the vertical distribution of isoprene. *Andronache et al.* [1994] and *Guenther et al.* [1996a, 1996b] have shown that isoprene varies significantly with altitude, even within a convective mixed layer. The model representation of vertical mixing, based on eddy diffusion, does not properly represent mixing processes within a convective layer [e.g., *Stull*, 1994; *Pleim and Chang*, 1992; *Hourdin et al.*, 2002]. The model isoprene in Figure 8 represents values for a vertical layer extending from 50 to ~600 m altitude in comparison with measured values at 500 m. Isoprene is expected to decrease with altitude over this range, and the next higher model layer (representing ~600–1200 m) has lower isoprene by a factor of 3. This suggests that the model underestimate of isoprene is somewhat larger than is shown in Figure 7. Other species (O_3, NO_x, anthropogenic VOCs) show little variation with altitude within the model convective mixed layer. Expressed as propene-equivalent carbon, measured isoprene represents 20% of total VOCs in the center of the Paris plume (1.4–3.7 ppbC isoprene, 11 ppbC anthropogenic VOCs) and 50% of total VOCs in the surrounding rural area.

[37] As shown in Tables 2 and 3, peak O_3 in the Paris plume does not change significantly when the isoprene emission rate in models is doubled. Increased isoprene emissions also have no impact on NO_x-VOC sensitivity for peak O_3 in the Paris plume. However, the spatial extent of the VOC-sensitive region in the Paris plume decreases by 40% in models with doubled isoprene emissions, as the shift

Table 4. Linear Least Squares Coefficients for VOCs Versus NO_y[a]

	17 July 1999 (1600 LST)			18 July 1999 (1600 LST)		
	a_0	a_1	r^2	a_0	a_1	r^2
Measured	1.2	.51	.78	1.7	.50	.82
Model scenario[b]						
Standard	−1.2	.56	.91	−2.2	.57	.81
Weekend adjustment	−1.3	.62	.90	−2.6	.67	.80
Modified VOCs	−2.1	.84	.91	−3.6	.86	.82
High VOCs, low NO_x	−3.2	1.3	.92	−5.3	1.3	.79

[a]Shown are the linear least squares estimators for the linear correlation [VOC] = $a_0 + a_1$[NO_y] from Figure 6 along with the correlation coefficient (r^2) from measurements and model scenarios. VOCs represent the sum of primary anthropogenic species as propene-equivalent carbon (ppbC).

[b]The model scenarios are: (1) the standard scenario; (2) a scenario with emissions adjusted based on weekend estimates from the work of *Vautard et al.* [2001]; (3) a scenario with anthropogenic VOC emissions increased by 40% relative to scenario 1; and (4) a scenario with anthropogenic emissions increased by 40% and NO_x decreased by 30% relative to scenario 1.

Table 5. Performance Statistics For 17 July[a]

	O_3		NO_y		VOCs		Isoprene	
Model Scenario[b]	Bias	Error	Bias	Error	Bias	Error	Bias	Error
Standard	−.02	.10	+.12	.38	−.21	.49	−.18	.73
High VOCs, low NO_x	−.04	.10	−.09	.23	+.19	.72	+.01	.81
High mixing height and VOCs	−.04	.09	+.01	.25	−.05	.53	−.16	.71

[a]The table shows normalized bias and normalized gross error between model and aircraft measurements for O_3, NO_y, summed primary VOCs (as propene-equivalent carbon), and isoprene on 17 July.

[b]The model scenarios are: (1) the standard scenario; (2) a scenario with anthropogenic emissions increased by 40% and NO_x decreased by 30% relative to scenario 1; and (3) a scenario with a 25% higher mixing height and higher VOCs.

to NO_x-sensitive conditions in the downwind plume occurs more rapidly.

[38] It is noteworthy that the statistics used for model evaluations in the U.S., normalized bias and normalized gross error, do not provide a strong basis for evaluating model accuracy. The U.S. EPA requires that models have normalized biases of <15% and normalized gross errors of <35%. All model scenarios meet these criteria for O_3, and all scenarios either meet or slightly exceed the criteria for NO_y (see Table 5). Evaluation based on the O_3-NO_y and VOC-NO_x correlations provides a more rigorous basis for evaluating the success of a model in representing the ozone formation process.

[39] A final issue concerns the impacts of wind speed and dilution on O_3-NO_x-VOC chemistry. Previously, *Milford et al.* [1994] and *Sillman* [1999] suggested that greater dilution (including higher wind speeds) should cause a shift toward greater sensitivity to NO_x rather than to VOCs. However, *Honoré et al.* [2000] found that higher wind speeds would lead to increased sensitivity to VOCs in box model calculations for Paris. In the model calculations shown here (Table 2), no significant change in NO_x-VOC sensitivity occurs in scenarios with wind speeds increased by 25%. When wind speeds are increased by 75%, peak O_3 in the Paris plume shows mixed sensitivity to NO_x and VOCs, whereas in the model base case, peak O_3 was strongly VOC-sensitive. The spatial extent of the VOC-sensitive region in the center of Paris also becomes smaller in the scenario with wind speeds increased by 75%. This result is consistent with the discussions by *Milford et al.* [1994] and *Sillman* [1999], although the impact of wind speed on NO_x-VOC sensitivity is small. The results from *Honoré et al.* [2000] may only be valid for extremely stagnant conditions in which air remains in a single metropolitan area for 2 days or longer.

6. Conclusions

[40] The above analysis of ozone, reactive nitrogen, and VOCs in the Paris urban plume has yielded a number of conclusions concerning ozone chemistry and O_3-NO_x-VOC sensitivity. Results from models and measurements both suggest that ozone in Paris is often close to the transition from NO_x-sensitive to VOC-sensitive chemistry. NO_x-VOC sensitivity in the Paris plume varies from day to day. The correlation between O_3 and NO_y in Paris is roughly comparable to that of Nashville during high-ozone events, and the O_3-NO_y slope is underestimated in models. Model reactivity-weighted VOCs are generally consistent with measurements, though with significant scatter. Measured isoprene is high enough to account for a significant portion of total VOC reactivity, even in the center of the Paris urban plume, but it has relatively little impact on ozone formation. Model-measurement comparisons for isoprene are especially difficult due to the uncertain vertical distribution of isoprene.

[41] The standard model scenario underestimates NO_y and the O_3/NO_y ratio in the center of the Paris plume and also underestimates the O_3-NO_y slope. This discrepancy appears in the O_3-NO_y correlation plots but is not obvious in the standard performance tests for ozone models, such as normalized bias. This type of discrepancy suggests that the model underestimates VOCs and/or VOC reactivity in the Paris plume possibly due to errors in emission inventories. Comparisons with measured VOCs do not support the hypothesis that VOC emissions are underestimated, but they do not rule out a possible underestimate of VOCs of up to 40%. The underestimated O_3-NO_y slope may be due to the presence of reactive VOCs in the Paris plume that were not included in the recent measurements. Alternately, the model-measurement discrepancy might be caused by loss of NO_y within the Paris plume (or within the measurement apparatus). Because the model-measurement discrepancy occurs at the center of the Paris plume rather than in the surrounding region, any such unknown VOC or removal of NO_y must be associated specifically with urban conditions.

[42] It is intriguing that on the days with high O_3, measured O_3 versus NO_y tends to agree with the model correlation only when the model predicts either NO_x-sensitive or transitional chemistry. As in previous studies of this type, the correlation between O_3 and NO_y in models is closely associated with model NO_x-VOC sensitivity predictions. The fact that model O_3/NO_y is lower than measured values in scenarios with VOC-sensitive chemistry provides some evidence that the VOC-sensitive scenarios may be incorrect.

[43] **Acknowledgments.** Discussions with Yves Balkansky, Daniel Martin, Bruno Nenninger, Nadege Blond, and Hauke Schmidt were especially helpful in preparing this manuscript. Support for this research was provided by the Centre National de la Recherche Scientifique and by the National Science Foundation (grants ATM-9713567 and ATM-0207841). The results may not necessarily reflect the views of the National Science Foundation, and no official endorsement should be inferred.

References

Andronache, C., W. L. Chameides, M. O. Rodgers, J. E. Martinez, P. Zimmerman, and J. Greenberg, Vertical distribution of isoprene in the lower boundary layer of the rural and urban southern United States, *J. Geophys. Res.*, *99*, 16,989–17,000, 1994.

Beekmann, M., and C. Derognat, Monte Carlo uncertainty analysis of a regional-scale transport chemistry model constrained by measurements from the Atmospheric Pollution Over the Paris Area (ESQUIF) campaign, *J. Geophys. Res.*, *108*, doi:10.1029/2003JD003391, in press, 2003.

Chameides, W. L., R. W. Lindsay, J. Richardson, and C. S. Kiang, The role of biogenic hydrocarbons in urban photochemical smog: Atlanta as a case study, *Science*, *241*, 1473–1474, 1988.

Chameides, W. L., et al., Ozone precursor relationships in the ambient atmosphere, *J. Geophys. Res.*, *97*, 6037–6056, 1992.

Derognat, C., M. Beekmann, M. Baeumle, D. Martin, and H. Schmidt, Effect of biogenic volatile organic compound emissions on tropospheric chemistry during the Atmospheric Pollution Over the Paris Area (ESQUIF) campaign in the Ile-de-France region, *J. Geophys. Res.*, *108*, doi:10.1029/2001JD001421, in press, 2003.

Gao, D., W. R. Stockwell, and J. B. Milford, Global uncertainty analysis of a regional-scale gas phase chemical mechanism, *J. Geophys. Res.*, *101*, 9102–9107, 1996.

Guenther, A., P. Zimmerman, L. Klinger, J. Greenberg, C. Ennis, K. Davis, W. Pollock, H. Westberg, G. Allwine, and C. Geron, Estimates of regional natural volatile organic compound fluxes from enclosure and ambient measurements, *J. Geophys. Res.*, *101*, 1345–1360, 1996a.

Guenther, A., et al., Isoprene fluxes measured by enclosure, relaxed eddy accumulation, surface layer gradient, mixed layer gradient, and mixed layer mass balance techniques, *J. Geophys. Res.*, *101*, 18,555–18,568, 1996b.

Honoré, C., R. Vautard, and M. Beekmann, Photochemical regimes in urban atmospheres: The influence of dispersion, *Geophys. Res. Lett.*, *27*, 1895–1898, 2000.

Hourdin, F., F. Couvreux, and L. Menut, Parameterization of the dry convective boundary layer based on a mass flux representation of thermals, *J. Atmos. Sci.*, *59*, 1104–1123, 2002.

Kanter, H. J., V. A. Mohnen, A. Volz-Thomas, W. Junkermann, K. Glaser, and H. Weitkamp, Integrated quality assurance in TSF for inorganic compounds (VOC): An overview on emission, physiology and ecology, *J. Atmos. Chem*, *33*, 23–88, 2001.

Konrad, S., and A. Volz-Thomas, Characterization of a commercial gas chromatography-flame ionization detection system for the in situ determination of C5–C10 hydrocarbons in ambient air, *J. Chromatogr. A*, *878*, 215–234, 2000.

Lattuati, M., Impact des emissions europeennes sur le bilan d'ozone tropospherique a l'interface de l'Europe et de l'Atlantique Nord: Apport de la modelisation lagrangienne et des meusres en altitude (in French), Ph.D. thesis, Univ. Paris VI, France, 1997.

Lu, C.-H., and J. S. Chang, On the indicator-based approach to assess ozone sensitivities and emissions features, *J. Geophys. Res.*, *103*, 3453–3462, 1998.

Martilli, A., A. Neftel, G. Favaro, F. Kirchner, S. Sillman, and A. Clappier, Simulation of the ozone formation in the northern part of the Po Valley, *J. Geophys. Res.*, *107*(D22), 8195, doi:10.1029/2001JD000534, 2002.

McClenny, W. A., (Ed.), Recommended methods for ambient air monitoring of NO, NO_2, NO_y, and individual NO_z species, *Rep. 600/R-01/005*, U.S. Envrion. Prot. Agency, Washington, D. C., 2000.

Menut, L., R. Vautard, M. Beekmann, and C. Honoré, Sensitivity of photochemical pollution using the adjoint of a simplified chemistry-transport model, *J. Geophys. Res.*, *105*, 15,379–15,402, 2000a.

Menut, L., et al., urements and modeling of atmospheric pollution over the Paris area: An overview of the ESQUIF project, *Ann. Geophys.*, *18*, 1467–1481, 2000b.

Milford, J., D. Gao, S. Sillman, P. Blossey, and A. G. Russell, Total reactive nitrogen (NO_y) as an indicator of the sensitivity of ozone to reductions in hydrocarbon and NO_x emissions, *J. Geophys. Res.*, *99*, 3533–3542, 1994.

Parrish, D. D., and F. C. Fehsenfeld, Methods for gas-phase measurements of ozone, ozone precursors and aerosol precursors, *Atmos. Environ.*, *34*, 1921–1957, 2000.

Pleim, J. E., and J. S. Chang, A non-local closure model for vertical mixing in the convective boundary layer, *Atmos. Environ., Part A*, *26*, 965–982, 1992.

Schmidt, H., C. Derognat, R. Vautard, and M. Beekmann, A comparison of simulated and observed ozone mixing ratios for the summer of 1998 in western Europe, *Atmos. Environ.*, *35*, 6277–6297, 2001.

Sillman, S., The use of NO_y, H_2O_2, and HNO_3 as indicators for O_3-NO_x-hydrocarbon sensitivity in urban locations, *J. Geophys. Res.*, *100*, 14,175–14,188, 1995.

Sillman, S., The relation between ozone, NO_x and hydrocarbons in urban and polluted rural environments, *Millenial Rev. Ser., Atmos. Environ.*, *33*, 1821–1845, 1999.

Sillman, S., and D. He, Some theoretical results concerning O_3-NO_x-VOC chemistry and NO_x-VOC indicators, *J. Geophys. Res.*, *107*(D22), 4659, doi:10.1029/2001JD001123, 2002.

Sillman, S., et al., Phtochemistry of ozone formation in Atlanta, GA: Models and measurements, *Atmos. Environ.*, *29*, 3055–3066, 1995.

Sillman, S., D. He, C. Cardelino, and R. E. Imhoff, The use of photochemical indicators to evaluate ozone-NO_x-hydrocarbon sensitivity: Case studies from Atlanta, New York and Los Angeles, *J. Air Waste Manage. Assoc.*, *47*, 642–652, 1997.

Sillman, S., D. He, M. R. Pippin, P. H. Daum, D. G. Imre, L. I. Kleinman, J. H. Lee, and J. Weinstein-Lloyd, Model correlations for ozone, reactive nitrogen, and peroxides for Nashville in comparison with measurements: Implications for O_3-NO_x-hydrocarbon sensitivity, *J. Geophys. Res.*, *103*, 22,629–22,644, 1998.

Simpson, D., Biogenic emissions in Europe: 2. Implications for ozone control strategies, *J. Geophys. Res.*, *100*, 22,891–22,906, 1995.

Simpson, D., et al., ntorying emissions from nature in Europe, *J. Geophys. Res.*, *104*, 8113–8152, 1999.

Staffelbach, T., et al., *J. Geophys. Res*, *102*, 23,345–23,362, 1997a.

Staffelbach, T., A. Neftel, and L. W. Horowitz, Photochemical oxidant formation over southern Switzerland: 2. Model results, *J. Geophys. Res.*, *102*, 23,363–23,374, 1997b.

Stohl, A., E. Williams, G. Wotawa, and H. Kromp-Kolb, A European inventory of soil nitric oxide emissions and the effect of these emissions on the photochemical formation of ozone in Europe, *Atmos. Environ.*, *30*, 3741–3755, 1996.

Stull, R. B., A convective transport theory for surface fluxes, *J. Atmos. Sci.*, *51*, 3–22, 1994.

Tonnesen, G. S., and R. L. Dennis, Analysis of radical propagation efficiency to assess ozone sensitivity to hydrocarbons and NO_x: 2. Long-lived species as indicators of ozone concentration sensitivity, *J. Geophys. Res.*, *105*, 9227–9241, 2000.

Vautard, R., M. Beekmann, J. Roux, and D. Gombert, Validation of a hybrid forecasting system for the ozone concentrations over the Paris area, *Atmos. Environ.*, *35*, 2449–2461, 2001.

Vautard, R., D. Martin, M. Beekmann, R. Friedrich, A. Jaubertie, D. Kley, M. Lathuati, P. Moral, B. Neininger, and J. Theolke, Paris emission inventory diagnostics from Atmospheric Pollution Over the Paris Area (ESQUIF) airborne measurements and a chemistry transport model, *J. Geophys. Res.*, *108*, doi:10.1029/2002JD002797, in press, 2003.

Verwer, J. G., and D. Simpson, Explicit methods for stiff ODEs from atmospheric chemistry, *Appl. Numer. Math.*, *18*, 413–430, 1995.

D. Kley, Forschungszentrum, D-52425 Jülich, Germany. (d.kley@fz-juelich.de)

L. Menut, Laboratoire Inter-Universitaire des Systèmes Atmosphériques, Centre National de la Recherche Scientifique, 61, avenue du Gal De Gaulle, F-91010 Créteil, France. (menut@lisa.univ-paris12.fr)

S. Sillman, Department of Atmospheric, Oceanic, and Space Sciences, University of Michigan, 2455 Hayward Street, Room 1541C SRB, Ann Arbor, MI 48109-2143, USA. (sillman@umich.edu)

R. Vautard, Laboratoire de Meteorologie Dynamique, Ecole Polytechnique, F-91128 Palaiseau, France. (vautard@lmd.polytechnique.fr)